The $He^{+\cdot}$ + CH_3CN Charge-Exchange Reaction: A Combined Semi-empirical and Quantum Chemical Study

Luca Mancini[1(✉)], Emília Valença Ferreira de Aragão[1], Fernando Pirani[1,2], Marzio Rosi[2,4], Noelia Faginas-Lago[1,4], and Daniela Ascenzi[3]

[1] Dipartimento di Chimica, Biologia e Biotecnologie, Università degli Studi di Perugia, 06123 Perugia, Italy
luca.mancini@unipg.it
[2] Dipartimento di Ingegneria Civile ed Ambientale, Università degli Studi di Perugia, 06125 Perugia, Italy
[3] Dipartimento di Fisica, niversità di Trento, Trento, Italy
[4] Istituto CNR di Scienze e Tecnologie Chimiche "Giulio Natta" (CNR-SCITEC), 06123 Perugia, Italy

Abstract. The reaction with the $He^{+\cdot}$ cation is considered one of the most important processes in the destruction of interstellar complex organic molecules (iCOMs). The development of accurate astrochemical databases requires the detailed knowledge of the rate constants and branching ratios of the processes. The dynamics of the charge exchange process between $He^{+\cdot}$ and methyl cyanide (CH_3CN) can be studied through a Landau-Zener-St*ü*ckelberg approach, which needs a detailed analysis of the potential energy surface (PES). In the present contribution, the Improved Lennard-Jones (ILJ) formulation is used to unveil the main features of the PES for $He^{+\cdot}$ + CH_3CN reaction, in order to set the stage for an accurate investigation of the dynamics of the charge-exchange process. The low computational cost and the high portability of the ILJ formulation allows to extend the approach to the study of different systems, with relevance in several fields, ranging from astrochemistry to nanomaterials.

Keywords: Astrochemistry · Improved Lennard-Jones · Reaction Dynamics · Theoretical Chemistry · Force Field

1 Introduction

Interstellar complex organic molecules (iCOMs), defined as organic molecules containing at least 6 atoms [1], have been detected through different stages of stellar evolution, from pre-stellar clouds to protostars and protoplanetary disks, and they act as important tracers of the physical conditions and of the evolution of the regions where they are observed. For an updated list of interstellar

© The Author(s), under exclusive license to Springer Nature Switzerland AG 2024
O. Gervasi et al. (Eds.): ICCSA 2024 Workshops, LNCS 14818, pp. 39–54, 2024.
https://doi.org/10.1007/978-3-031-65273-8_3

and circumstellar molecules, now comprising over 300 species [2], see the Cologne Database for Molecular Spectroscopy [3–5]. The correct implementation of astrochemical models, built to reproduce the observed iCOM abundances, strongly depends on the kinetics of the chemical reactions implemented as possible formation and destruction mechanisms of iCOMs. To this purpose astrochemical databases (*e.g.* the KIDA [6] and UMIST [7,8] databases) are widely used to obtain kinetic parameters and there is a strong need to keep such databases updated with the most recent experimental/theoretical estimates of rate coeffcients and branching ratios.

A particular class of interstellar molecules is represented by nitriles, a set of N-bearing organic compounds, which accounts for ca. 15 % of the total species detected in the interstellar medium (ISM) [9] and represent an interesting category of compounds in prebiotic chemistry [10], being possible precursors of complex structures of amino acids and RNA [11–13]. Acetonitrile (CH_3CN), one of the simplest nitriles, is also one of the most abundant iCOM observed. After the first detection towards the SgrB2 and SgrA molecular clouds [14], it has been revealed in different regions associated to various stages of the formation of stars and stellar systems [15–24] and in comets [25–27]. According to the main astrochemical databases, the most important destruction mechanisms of acetonitrile are due to collisions with ions, including $He^{+\cdot}$ (that is considered one of the main destruction routes for iCOMs), formed through the interaction of He atoms with cosmic rays. A detailed chemical investigation is therefore pivotal to unveil the reaction dynamics and derive the rate constant of the process.

To this purpose, a theoretical analysis can help to elucidate the main features of the potential energy surface (PES) which triggers the dynamics of the charge-exchange process. In this respect, semi-empirical models represent a feasible and accurate method to treat non-covalent interactions and provide useful parameters for the development of the PES, given in a proper analytical form, which is a necessary condition to perform molecular dynamics simulations. Among them, the Improved Lennard-Jones (ILJ) functional [28] has been developed in order to have a refined analysis of both long-range attraction and short-range repulsion. Recently, the ILJ formulation has been used to investigate the long range component of the interaction in the case of bimolecular (neutral-neutral and ion-neutral) gas-phase reactions [29–31], helping to elucidate the reaction mechanism at the microscopic level. Additionally, the ILJ formulation represents a feasible method, characterized by a high degree of portability and low computational demand. Therefore, it can be used for several purposes, ranging from astrochemistry and reaction dynamics to material sciences, including the development of new generation nano-materials for energy storage and carbon neutrality. In the present contribution, the ILJ potential has been used, in conjunction with *ab initio* calculations, to study the PES for the $He^{+\cdot}$ + CH_3CN reaction, in order to provide the building blocks for the complete treatment of the reaction dynamics.

2 Theoretical Methods

2.1 Electronic Structure Calculations

Electronic structure calculations have been performed in order to derive the main geometrical parameters of the interacting systems. The geometry of the CH_3CN molecule has been optimized using Density Functional Theory (DFT) calculations, with the B3LYP functional [32,33], together with the correlation consistent valence polarized set aug-cc-pVTZ [34–36]. The same computational strategy has been used to calculate harmonic vibrational frequencies, in order to check the nature of the stationary point, as well as the Mulliken atomic charges. Finally, the same level of theory has been used to perform an analysis of the atomic orbitals, in order to derive the shape and the energy of the molecular orbitals (MO's), to be used in the dynamical effects treatment of the interaction with $He^{+\cdot}$.

2.2 Semi-empirical Analysis of the Non-covalent Interactions

The non-covalent interaction between the $He^{+\cdot}$ radical cation and CH_3CN has been analysed adopting a strategy already used for similar systems [29,37,38]. In details, the PES has been built for both the entrance ($He^{+\cdot}$ + CH_3CN) and the exit (He + $CH_3CN^{+\cdot}$) channels. The PES is given in an analytical form and depends on the distance (defined as R) between $He^{+\cdot}$ (or He in the case of the exit channel) and the center of mass of the acetonitrile molecule (or its radical cation, for the exit channel), and on the relative orientation of the involved partners. In this respect, it is important to notice that, due to the symmetry of the CH_3CN molecule, the relative orientation can be defined considering only θ, which is the angle defined by the $\mathbf{R}$ vector and the z axis (taken to coincide with the C_{3v} symmetry axis of CH_3CN).

In order to have a simpler representation of the system, CH_3CN has been represented considering three moieties: the C and N atoms of the cyano group and an effective atom (indicated as C_{eff}), having the mass and polarizability of a methyl group (CH_3). The global potential describing the interaction is composed of two contributions: a first term representing the electrostatic potential (V_{elect}) and a second term (V_{nelect}), accounting for the non electrostatic contribution of the interaction.

PES feature of the entrance channel:

For the **entrance channel**, the electrostatic term is defined as:

$$V_{elect}(R,\theta) = 14400 \cdot \left(\frac{q_C}{r_C} + \frac{q_N}{r_N} + \frac{q_{C_{eff}}}{r_{C_{eff}}} \right) \tag{1}$$

where q_C, q_N and $q_{C_{eff}}$ are the effective atomic charges, calculated as in Sect. 2.1. The variables r_C, r_N and $r_{C_{eff}}$ represent the distances between one of the three moieties (C, N, C_{eff}) of CH_3CN and $He^{+\cdot}$, evaluated by exploiting the Carnot's theorem. In details, considering the reference system reported in Fig. 1, the three distances are formulated as:

$$r_C^2 = R^2 + d_C^2 - 2R \cdot d_C \cdot cos\theta \tag{2}$$

$$r_N^2 = R^2 + d_N^2 - 2R \cdot d_N \cdot cos\theta \tag{3}$$

$$r_{C_{eff}}^2 = R^2 + d_{C_{eff}}^2 - 2R \cdot d_{C_{eff}} \cdot cos(\pi - \theta) \tag{4}$$

where d_C, d_N and $d_{C_{eff}}$ are the distances between the CM (at the axes origin) and the position of the C, N and C_{eff} atoms/effective atoms within the CH_3CN molecule . The factor 14400 allows to obtain $V_{elect}(R,\theta)$ in meV when the charges are given in atomic units and the distances in $\mathring{A}$.

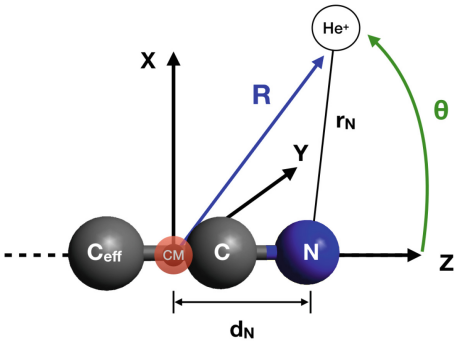

Fig. 1. Coordinate system used for the representation of the (He - CH_3CN)$^+$ system. For simplicity, only the relation between r_N and R, θ is reported, while the other parameters are defined in the same way.

The non-electrostatic contribution has been evaluated considering the Improved Lennard-Jones (ILJ) model [28,39–41] formulation. V_{nelect} is defined as balance of size repulsion contributions, dominant at short distance, with induction and dispersion attraction contributions, prevalent at large intermolecular

distances. Such balance is obtained as additivity of components due to the interaction of $He^{+\cdot}$ with the three effective atoms of the molecule (C, N and C_{eff}). Each component is described by an ILJ function (V_{ILJ}), a simple-reliable potential model that simultaneously includes the combination of the long-range attraction with short-range repulsion effects. For any of the three pairs, interacting at a separation distance r (with r equal to r_C, r_N or $r_{C_{eff}}$, according to the moiety under consideration) the general formulation of V_{ILJ} is:

$$V_{ILJ}(r) = \varepsilon \left[\frac{m}{n(r) - m} \left(\frac{r_m}{r} \right)^{n(r)} - \frac{n(r)}{n(r) - m} \left(\frac{r_m}{r} \right)^{m} \right] \tag{5}$$

where, for each interaction pair, ε and r_m represents the well depth of the potential and its location, respectively, while the ratio r_m/r is the reduced distance. The ε and r_m values are estimated on the basis of the polarizability components associated to each interacting pair. For an ion-neutral pair the m parameter is equal to 4, while the $n(r)$ term, that modulates both strength and radial dependence of the repulsion and the strength of the attraction, is expressed considering the hardness of the two interacting fragments, taken into account in the β parameter:

$$n(r) = \beta + 4 \left(\frac{r}{r_m} \right)^2 \tag{6}$$

Therefore, in the entrance channel the overall non electrostatic component is the sum of three contributions:

$$V_{nelect}(R, \theta) = V_{ILJ}(r_C) + V_{ILJ}(r_N) + V_{ILJ}(r_{C_{eff}}) \tag{7}$$

For all the interacting pairs the relevant parameters are given in Sect. 3.2.

PES feature of the exit channel:

The PES in the exit channel arises from a balance between a long range attraction, due to dispersion and induction components, and a short range repulsion, associated to size effects. The combination of the dispersion attraction and size repulsion effects is defined as a van der Waals interaction, V_{vdW}, which is expressed, similarly to what already done for the entrance channel, in terms of three V'_{ILJ} functions, one for each interaction pair due to He and each effective atom of $CH_3CN^{+\cdot}$ molecular ion:

$$V_{vdW}(R, \theta) = V'_{ILJ}(r_C) + V'_{ILJ}(r_N) + V'_{ILJ}(r_{C_{eff}}) \tag{8}$$

For such pairs, m has been fixed to 6, to correctly represent the asymptotic behaviour of the dispersion. The potential parameters associated with the three different V'_{ILJ} contributions are reported in Sect. 3.2. It should be emphasized that the $CH_3CN^{\cdot +}$ molecular ion is formed in an excited state, by ejection of one electron from one of the inner valence MO's, as it will be detailed in Sect. 3.1. As a consequence, its electronic polarizability, mostly determined by the behaviour

of electrons populating outer MO's, is assumed to be the same of the neutral CH_3CN and it is therefore partitioned in the same way.

Additionally, a component V_{ind} has been added, to take into account the ion-induced dipole contribution, not directly enclosed in V_{vdW}, and whose strength is comparable with that of the dispersion. Such component depends on the separation distance R between the He atom and the CM of the molecular cation $CH_3CN^{+\cdot}$. Therefore V_{ind} is formulated, considering the polarizability α of He (equal to 0.2 $Å^3$) and expressing R in units of Å, by the semi-empirical relation:

$$V_{ind}(R) = -7200\frac{\alpha_{He}}{R^4} \tag{9}$$

where the factor 7200 provides V_{ind} in meV units.

3 Results

3.1 Electronic Structure Calculations

In Fig. 2, the optimized geometry obtained for the acetonitrile molecule is reported, including bond distances (in Å) and angles (in degrees). The distances obtained at the B3LYP/aug-cc-pVTZ level of theory can be compared with the data reported in the NIST database [42], showing a very good agreement. The main deviation is indeed represented by the C-H bond length, which is reported to be equal to 1.104 Å (differing by 0.015 Å from the calculated data). As already noticed in the analysis of previous systems [43–47], the proposed methodology can be considered a good approximation balancing between chemical accuracy and computational cost.

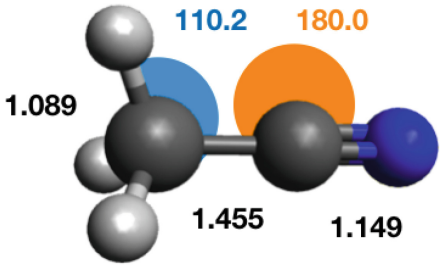

Fig. 2. Bond distances (in black, in Å) and angles (in colours, in degrees) for the CH_3CN molecule obtained at the B3LYP/aug-cc-pVTZ level of theory.

The optimized geometry has been used as a starting point for the analysis of the molecular orbitals of the system. In Table 1, the energies of some of the MO's calculated for the CH_3CN molecule are reported.

Table 1. Energies (in eV) calculated for the main MO's of the CH_3CN molecule necessary for the analysis of the charge-exchange process. The zero level is represented by the electron separated from the molecule.

Molecular Orbital	Energy (eV)
LUMO	0.643
HOMO	–11.420
HOMO-5	–16.555
HOMO-6	–23.988
HOMO-7	–27.569

The results obtained must be compared with the ionization energy of the He atom, equal to 24.587 eV [48], the highest value in the whole Periodic Table. As a consequence, an electron transfer from the HOMO or HOMO-5 to the 1*s* atomic orbital of $He^{+\cdot}$ would be highly exothermic (see the data reported in Table 1), and such large differences in the asymptotic values of the entrance and exit PESs would lead to an inefficient non-adiabatic coupling between the entrance and exit PESs at distances that are relevant for the electron transfer. As a consequence, the best candidate for the charge exchange via non-adiabatic coupling of the PESs appears to be the HOMO-6 orbital, having an energy of -23.998 eV. Figure 3 shows the shapes of the main MO's considered in the analysis. As can be seen, the HOMO-6 orbital involved in the charge exchange process is characterized by the presence of a nodal plane in correspondence of the C atom of the cyano group.

It should be noted that the energies of the MO's obtained at the DFT level of theory provide only an estimation of the ionization energy and have been used to establish which is the orbital involved in the ionization process. In absence of clear experimental data we decided to rely on the results coming from the DFT analysis which provides values closer to the accurate ones, without making use of multi-reference methods, which are extremely costly in terms of CPU time and disk space requirements.

In Table 2 are reported the effective atomic charges (q) calculated for the three moieties in which the CH_3CN molecule has been partitioned. The CH_3CN molecule is a symmetric top rotor that exhibits rotational components both along its C_{3v} symmetry axis, where is aligned its high permanent electric dipole (3.919 D), and perpendicular to it. As previously reported (see Sect. 2.2), the molecule can be considered as formed by three effective atoms. The polarizability of CH_3CN (equal to 4.30 Å^3), is partitioned in three effective components, one assigned to C_{eff} (equal to 2.20 Å^3), another assigned to C (1.00 Å^3), and the third associated to N (1.10 Å^3). The partial charges calculated for CH_3CN, and reported in Table 2, appear to be consistent with its permanent electric dipole and quadrupole moment. In Table 3 are reported the ILJ parameters used for to derive the PES for the entrance and exit channel.

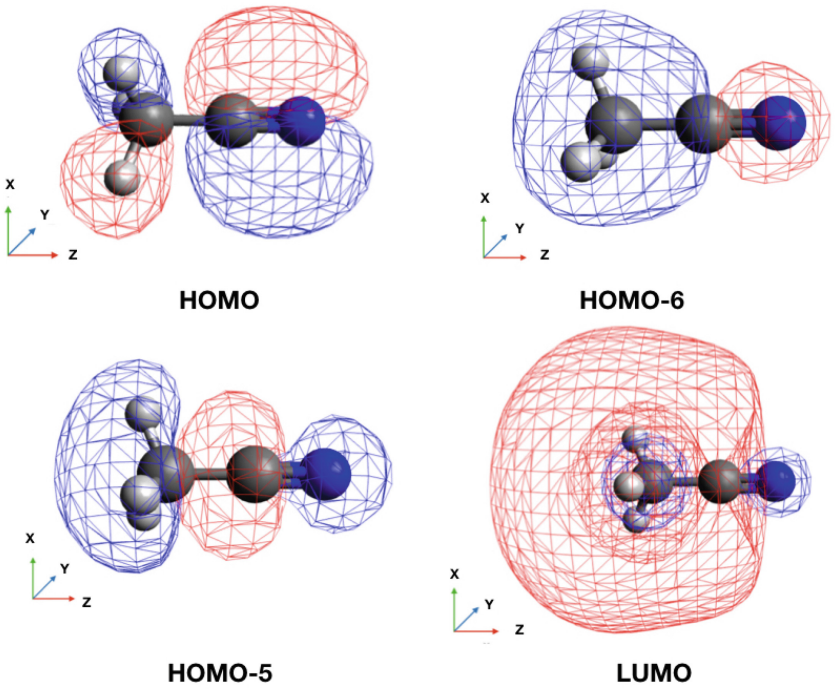

Fig. 3. Shape of the main MO's for the CH_3CN molecule, obtained at the B3LYP/aug-cc-pVTZ level of theory. Blue regions indicate the positive densities, while red regions are the negatively charged ones. (Color figure online)

Table 2. Atomic charges (q) obtained for the CH_3CN molecule, evaluated at the B3LYP/aug-cc-pVTZ level of theory. The charge of C_{eff} is representative of the methyl group and calculated considering the atomic charge of C and three atomic charges of H atoms.

Atom	**Charge q (a.u.)**
C	0.4501
N	–0.5006
C_{eff}	0.0505

Table 3. List of the ILJ parameters, used in Eq. 5 and 6, derived for the modeling of the non-covalent interaction in both the entrance and exit channel.

interacting pairs	r_m**(Å)**	ϵ **(meV)**	**m**	β
Entrance channel				
$He^{+\cdot}$ - C_{eff}	2.58	312	4	7
He^+ - C	2.31	189	4	7
$He^{+\cdot}$ - N	2.33	198	4	7
Exit channel				
He - C_{eff}	3.69	2.3	6	8
He - C	3.30	2.1	6	8
He - N	3.33	2.2	6	8

3.2 PES in the Entrance and Exit Channel

The data obtained through the analysis reported in Sect. 2.2 have been used to calculate the analytical PES for the entrance and exit channels. To provide an easier representation of the interacting system, polar coordinates are employed. Specifically, the CH_3CN molecule (and consequently the $CH_3CN^{+\cdot}$ radical cation) exhibit cylindrical symmetry. As a consequence (as mentioned above), the potential representing the interaction can be described using only two coordinates: R (the distance between the $He^{+\cdot}$ cation and the CM of the CH_3CN molecule) and θ, representing the angle between the **R** vector and the z axis. This significantly reduces the complexity of the treatment. Figure 4 shows some cuts of the entrance PES for specific values of θ angle.

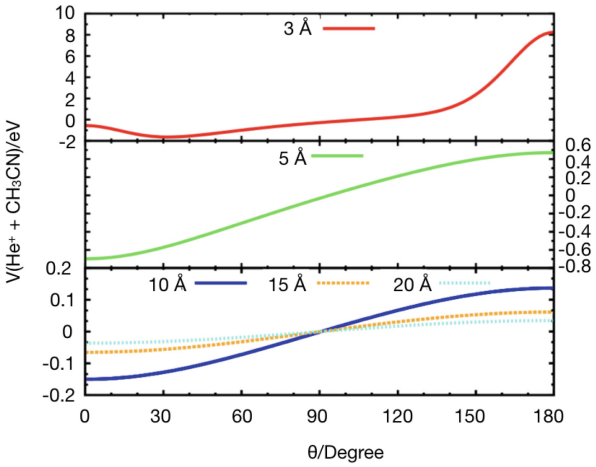

Fig. 4. Cuts of the PES for the $He^{+\cdot}$ + CH_3CN entrance channel for five different values of R, as a function of θ

As observed from the cuts reported in Fig. 4, entrance barriers are evident, with heights increasing as R decreases. These barriers, under thermal and sub-thermal conditions, are insurmountable due to the rotational motion of the CH_3CN molecule, which changes the θ angle. Consequently, the rotational component perpendicular to the C_3v axis is significantly hindered during the collision event. In Fig. 5 some cuts of the PES in the exit channel are presented.

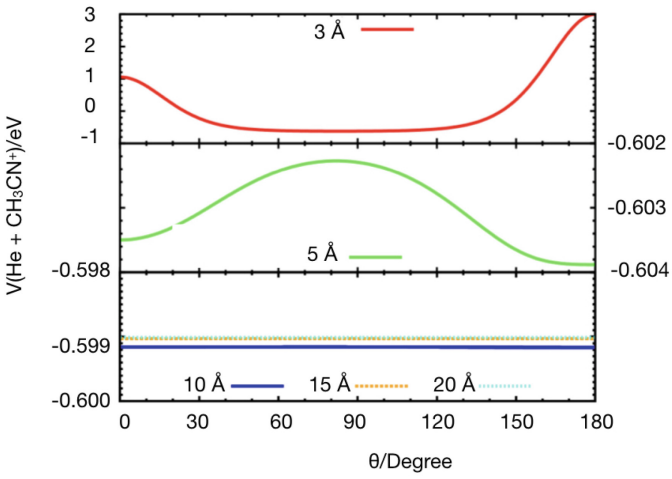

Fig. 5. Cuts of the PES for the He + $CH_3CN^{+\cdot}$ exit channel for five different values of R, as a function of θ

To properly characterize the reaction dynamics, it is pivotal to analyze the *non-adiabatic transitions* at the crossing between the entrance and exit channel of the PES, which are located in a wide range of separation distances. Additionally, the significant disparity in the ionization energy (IE) of the two species (IE_{He}= 24.587 eV and IE_{CH3CN} = 12.20 ± 0.01 eV [48]) does not permit a crossing between the entrance and exit channels in the case of an electron being ejected by the HOMO of CH_3CN. In Fig. 6, the crossing points between the entrance $He^{+\cdot}$ – CH_3CN (green curves) and exit He – $CH_3CN^{\cdot+}$ (red continuous curve) channels are illustrated for six different orientations, determined by θ values equal to 0°, 25°, 50°, 75°, 90° and 110° with the CH_3CN radical cation formed in its electronic ground state. Additionally, the red dashed curves represent the exit channels assuming the removal of an electron from the inner valence orbital HOMO-6.

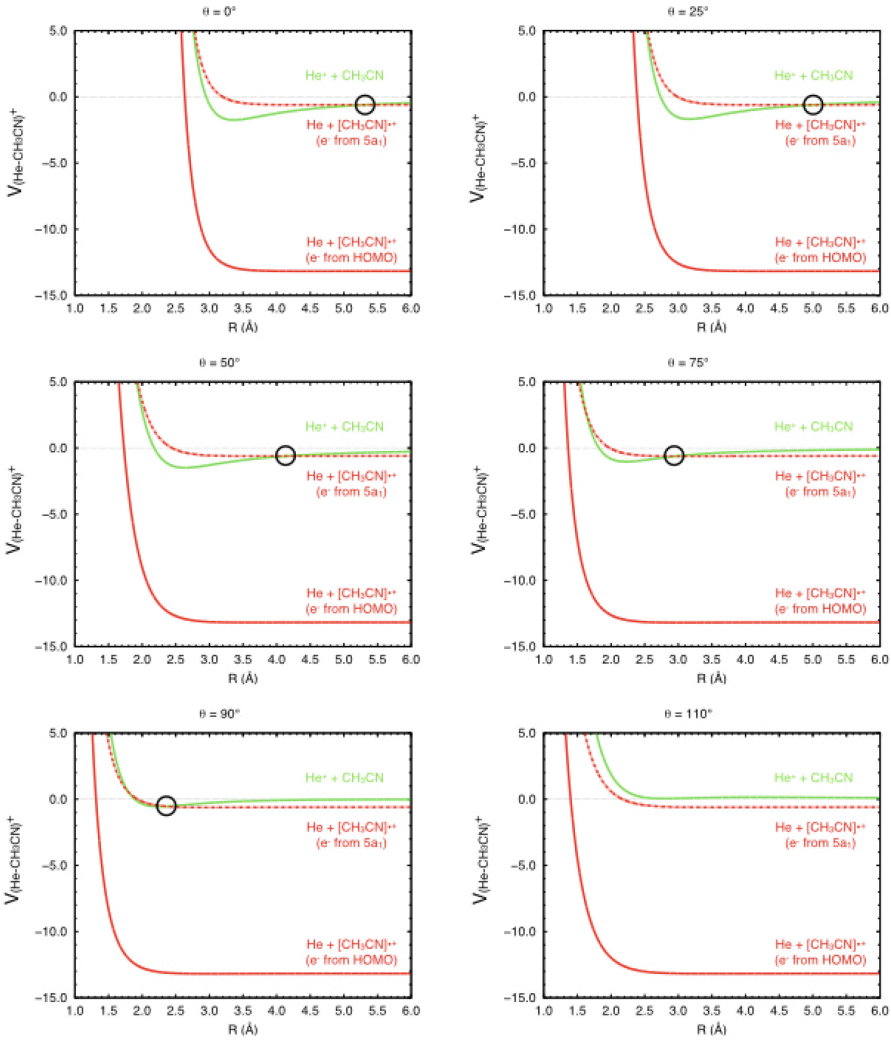

Fig. 6. PES crossings: PE curves of the entrance $He^+ - CH_3CN$ (green curves) and exit $He - CH_3CN^{\cdot+}$ (red continuous curve) channels for six different orientation determined by θ values equal to 0°, 25°, 50°, 75°, 90° and 110° with the CH_3CN radical cation formed in its electronic ground state. The red dashed curves represent exit channels assuming the removal of an electron from the HOMO-6 orbital (indicated in figure as $5a_1$, according to the photoelectron spectra).

As emphasized above, in order to have effective crossings between entrance and exit interaction potentials, the electron must be removed from an inner orbital, with a higher ionization potential. Photoelectron spectra [49] and the present electronic state calculations suggest that the inner valence molecular

orbital HOMO-6, is the one having an energy comparable with the IE of He, thus being the proper MO to promote the electron exchange process. The experimental findings are in agreement with the energy of the MO calculated (and reported above). Assuming the IE of HOMO-6 (indicated as $5a_1$ in the photoelectron spectra of acetonitrile [49]) as the proper asymptotic level for the exit channels, a sequence of crossings is obtained (see the red dashed lines in Figs. 6) where *non-adiabatic* charge transfer effects are essential to trigger the ion-molecule reaction. It is of relevance to note that the most effective crossing points manifest for θ varying from 0° up to about 90°, while no crossings occur for θ significantly larger than 90°.

4 Conclusions

In this study, a theoretical investigation of the interaction between the $He^{+\cdot}$ radical cation and the CH_3CN molecule has been conducted to offer valuable insights for future analysis of the dynamics involved in the charge exchange process, which is particularly significant in astrochemical models. Reactions involving cosmic rays generated $He^{+\cdot}$ ions are indeed among the primary destruction mechanisms proposed for iCOMs.

The method proposed here involves a phenomenological approach to construct the PESs, in an analytical form, for the entrance and exit channels of the reactions, namely $He^{+\cdot}$ + CH_3CN and He + $CH_3CN^{+\cdot}$. The phenomenological approach identifies the primary interaction components and describes them exploiting empirical or semi-empirical formulas defined by a limited number of parameters, *e.g.* via semi-empirical Improved-Lennard Jones potentials. These potential parameters can be adjusted within a restricted range of variation since they are linked to fundamental chemico-physical properties of the interacting partners, such as electronic polarizabilities (which can be partitioned into atomic and group components), ionization potentials, electron affinity, permanent charges, anisotropic charge distributions determining permanent electric multipoles, energy and shape of the atomic and molecular orbitals involved in charge (electron) transfer effects (CT). The next step of the treatment involves an accurate investigation of the reaction dynamics. In particular, the PESs presented in this work will enable the identification of a series of crossings between entrance and exit channels where the reactive process is triggered by non-adiabatic couplings due to the charge transfer process. Subsequently, the Landau-Zener-Stückelberg approach will be employed to evaluate the crossing probability and, ultimately, the reactive cross sections. Guided ion beam scattering experiments involving $He^{+\cdot}$ - CH_3CN collisions have recently been conducted in the laboratories of the University of Trento, and the analysis of the experimental findings, exploiting the results of this study, is currently underway.

Acknowledgements. This work has been funded by the European Union - NextGenerationEU under the Italian Ministry of University and Research (MUR) National Innovation Ecosystem grant ECS00000041 - VITALITY - CUP J97G22000170005. N. Faginas Lago and M. Rosi also acknowledge financial support under the National Recovery and Resilience Plan (NRRP), Mission 4, Component 2, Investment 1.1, Call for tender No. 104 published on 2.2.2022 by the Italian Ministry of University and Research (MUR), funded by the European Union - NextGenerationEU- Project Title 2022JC2Y93 ChemicalOrigins: linking the fossil composition of the Solar System with the chemistry of protoplanetary disks - CUP J53D23001600006 - Grant Assignment Decree No. 962 adopted on 30.06.2023 by the Italian Ministry of Ministry of University and Research (MUR). D. Ascenzi acknowledges financial support from European Union's Horizon 2020 research and innovation programme under the Marie Sklodowska Curie grant agreement N. 811312 (project 'Astro-Chemical Origins' ACO), from MUR PRIN 2020 project n. 2020AFB3FX 'Astrochemistry beyond the second period elements' and from the National Recovery and Resilience Plan (NRRP), Mission 4, Component 2, Investment 1.1, Call for tender No. 1409 published on 14.9.2022 by the Italian Ministry of University and Research (MUR), funded by the European Union - NextGenerationEU- Project Title P20223H8CK Degradation of space-technology polymers by thermospheric oxygen atoms and ions: an exploration of the reaction mechanisms at an atomistic level - CUP E53D23015560001. Views and opinions expressed are however those of the author(s) only and do not necessarily reflect those of the European Union or European Commission. Neither the European Union nor the granting authority can be held responsible for them.

References

1. Herbst, E., Van Dishoeck, E.F.: Complex organic interstellar molecules. Ann. Rev. Astron. Astrophys. **47**, 427–480 (2009)
2. McGuire, B.A.: 2021 census of interstellar, circumstellar, extragalactic, protoplanetary disk, and exoplanetary molecules. Astrophys. J. Suppl. Ser. **259**(2), 30 (2022)
3. Müller, H.S.P., Thorwirth, S., Roth, D.A., Winnewisser, G.: The cologne database for molecular spectroscopy. CDMS. Astron. Astrophys. **370**, L49–L52 (2001)
4. Müller, H.S.P., Thorwirth, S., Roth, D.A., Winnewisser, G.: The cologne database for molecular spectroscopy, CDMS: Useful tool for astronomers and spectroscopists. J. Mol. Struct. **742**, 215–227 (2005)
5. https://cdms.astro.uni-koeln.de/classic/
6. Wakelam, V., et al.: A kinetic database for astrochemistry (KIDA). Astrophys. J. Suppl. Ser. **199**(1), 21 (2012)
7. Millar, T.J., Walsh, C., de Sande, M.V., Markwick, A.J.: The UMIST database for astrochemistry 2022. Astron. Astrophys. **682**, A109 (2024). https://doi.org/10.1051/0004-6361/202346908
8. McElroy, D., Walsh, C., Markwick, A., Cordiner, M., Smith, K., Millar, T.: The UMIST database for astrochemistry 2012. Astron. Astrophys. **550**, A36 (2013)
9. Cabezas, C., et al.: The millimeter-wave spectrum and astronomical search of succinonitrile and its vibrational excited states. Astron. Astrophys. **629**, A35 (2019)
10. Brack, A.: The Molecular Origins of Life: Assembling Pieces of the Puzzle. Cambridge University Press (1998)
11. Zhao, Q., Garimella, S.S., Savoie, B.M.: Thermally accessible prebiotic pathways for forming ribonucleic acid and protein precursors from aqueous hydrogen cyanide. J. Am. Chem. Soc. **145**(11), 6135–6143 (2023)

12. Meisner, J., Zhu, X., Martínez, T.J.: Computational Discovery of the Origins of Life (2019)
13. Walker, S.I.: Origins of life: a problem for physics. arXiv preprint arXiv:1705.08073 (2017)
14. Solomon, P., Jefferts, K., Penzias, A., Wilson, R.: Detection of millimeter emission lines from interstellar methyl cyanide. Astrophys. J. vol. 168, p. L107 **168**, L107 (1971)
15. Matthews, H.E., Sears, T.J.: Detection of the j= 1-0 transition of CH3CN. Astrophys. J. Part 2-Lett. Editor, vol. 267, Apr. 1, 1983, p. L53–L57. **267**, L53–L57 (1983)
16. Minh, Y., Irvine, W.M., Ohishi, M., Ishikawa, S., Saito, S., Kaifu, N.: Measurement of the methyl cyanide E/A ratio in TMC-1. Astron. Astrophys. (ISSN 0004-6361), vol. 267, no. 1, p. 229–232. **267**, 229–232 (1993)
17. Megías, et al.: The complex organic molecular content in the L1517B starless core. Mon. Not. R. Astron. Soc. **519**(2), 1601–1617 (2023)
18. Vastel, C., Loison, J.C., Wakelam, V., Lefloch, B.: Isocyanogen formation in the cold interstellar medium. Astron. Astrophys. **625**, A91 (2019)
19. Cazaux, S., et al.: The hot core around the low-mass protostar IRAS 16293–2422: scoundrels rule! Astrophys. J. **593**(1), L51 (2003)
20. Bottinelli, S., et al.: Complex molecules in the hot core of the low-mass protostar NGC 1333 IRAS 4A. Astrophys. J. **615**(1), 354 (2004)
21. Calcutt, H., et al.: The ALMA-PILS survey: complex nitriles towards IRAS 16293–2422. Astron. Astrophys. **616**, A90 (2018)
22. Mercimek, S., et al.: Chemical survey of class i protostars with the IRAM-30 m. Astron. Astrophys. **659**, A67 (2022)
23. Bianchi, E., et al.: SOLIS-XV. CH3CN deuteration in the SVS13-A class i hot corino. Astron. Astrophys. **662**, A103 (2022)
24. Öberg, K.I., et al.: The comet-like composition of a protoplanetary disk as revealed by complex cyanides. Nature **520**(7546), 198–201 (2015)
25. Rodgers, S., Charnley, S.: Organic synthesis in the coma of comet hale-bopp? Mon. Not. R. Astron. Soc. **320**(4), L61–L64 (2001)
26. Le Roy, L., et al.: Inventory of the volatiles on comet 67P/churyumov-gerasimenko from rosetta/ROSINA. Astron. Astrophys. **583**, A1 (2015)
27. Biver, N., et al.: Observations of comet C/2020 F3 (NEOWISE) with IRAM telescopes. Astron. Astrophys. **668**, A171 (2022)
28. Pirani, F., Brizi, S., Roncaratti, L.F., Casavecchia, P., Cappelletti, D., Vecchiocattivi, F.: Beyond the lennard-jones model: a simple and accurate potential function probed by high resolution scattering data useful for molecular dynamics simulations. Phys. Chem. Chem. Phys. **10**(36), 5489–5503 (2008)
29. Richardson, V., et al.: Fragmentation of interstellar methanol by collisions with he˙+: an experimental and computational study. Phys. Chem. Chem. Phys. **24**(37), 22437–22452 (2022)
30. Marchione, D., et al.: Unsaturated dinitriles formation routes in extraterrestrial environments: a combined experimental and theoretical investigation of the reaction between cyano radicals and cyanoethene (C2H3CN). J. Phys. Chem. A **126**(22), 3569–3582 (2022)
31. Giani, L., et al.: Revised gas-phase formation network of methyl cyanide: the origin of methyl cyanide and methanol abundance correlation in hot corinos. Mon. Not. R. Astron. Soc. **526**(3), 4535–4556 (2023)

32. Becke, A.D.: A new mixing of Hartree-Fock and local density-functional theories. J. Chem. Phys. **98**(2), 1372–1377 (1993)
33. Stephens, P.J., Devlin, F.J., Chabalowski, C.F., Frisch, M.J.: Ab initio calculation of vibrational absorption and circular dichroism spectra using density functional force fields. J. Phys. Chem. **98**(45), 11623–11627 (1994)
34. Dunning Jr, T.H.: Gaussian basis sets for use in correlated molecular calculations. I. the atoms boron through neon and hydrogen. J. chem. phys. **90**(2), 1007–1023 (1989)
35. Woon, D.E., Dunning Jr, T.H.: Gaussian basis sets for use in correlated molecular calculations. III. the atoms aluminum through argon. J. chem. phys. **98**(2), 1358–1371 (1993)
36. Kendall, R.A., Dunning Jr, T.H., Harrison, R.J.: Electron affinities of the first-row atoms revisited. systematic basis sets and wave functions. J. chem. phys. **96**(9), 6796–6806 (1992)
37. Cernuto, A., Tosi, P., Martini, L.M., Pirani, F., Ascenzi, D.: Experimental investigation of the reaction of helium ions with dimethyl ether: stereodynamics of the dissociative charge exchange process. Phys. Chem. Chem. Phys. **19**(30), 19554–19565 (2017)
38. Cernuto, A., Pirani, F., Martini, L.M., Tosi, P., Ascenzi, D.: The selective role of long-range forces in the stereodynamics of ion-molecule reactions: The He++ methyl formate case from guided-ion-beam experiments. ChemPhysChem **19**(1), 51–59 (2018)
39. Liuti, G., Pirani, F.: Regularities in van der Waals forces: correlation between the potential parameters and polarizability. Chem. Phys. Lett. **122**(3), 245–250 (1985)
40. Pirani, F., Maciel, G.S., Cappelletti, D., Aquilanti, V.: Experimental benchmarks and phenomenology of interatomic forces: open-shell and electronic anisotropy effects. Int. Rev. Phys. Chem. **25**(1–2), 165–199 (2006)
41. Pirani, F., Albertı, M., Castro, A., Teixidor, M.M., Cappelletti, D.: Atom-bond pairwise additive representation for intermolecular potential energy surfaces. Chem. Phys. Lett. **394**(1–3), 37–44 (2004)
42. Johnson, R.D., et al.: NIST Computational Chemistry Comparison and Benchmark Database. http://srdatanist.gov/cccbdb (2006)
43. Vanuzzo, G., et al.: Reaction N(2D) + CH2CCH2 (Allene): an experimental and theoretical investigation and implications for the photochemical models of titan. ACS Earth Space Chem. **6**(10), 2305–2321 (2022)
44. Mancini, L., et al.: The reaction n (2d)+ CH3CCH (methylacetylene): a combined crossed molecular beams and theoretical investigation and implications for the atmosphere of titan. J. Phys. Chem. A **125**(40), 8846–8859 (2021)
45. Pannacci, G., et al.: A combined crossed molecular beam and theorerical study of the O (3 P, 1 D)+ acrylonitrile (CH 2 CHCN) reactions and implications for combustion and extraterrestrial environments. Phys. Chem. Chem. Phys. **25**(30), 20194–20211 (2023)
46. Vanuzzo, G., et al.: The N (2D)+ CH2CHCN (vinyl cyanide) reaction: a combined crossed molecular beam and theoretical study and implications for the atmosphere of titan. J. Phys. Chem. A **126**(36), 6110–6123 (2022)
47. Rosi, M., et al.: Possible scenarios for SiS formation in the interstellar medium: electronic structure calculations of the potential energy surfaces for the reactions of the SiH radical with atomic sulphur and S2. Chem. Phys. Lett. **695**, 87–93 (2018)

48. NIST Chemistry Webbook. NIST Standard Reference Database Number 69, Eds. P.J. Linstrom and W.G. Mallard, National Institute of Standards and Technology, Gaithersburg MD, 20899 https://webbook.nist.gov/chemistry/. March 26 2024
49. Asbrink, L., Von-Niessen, W., Bieri, G.: 30.4 nm He(D) Photoelectron Spectra of Organic Molecules. J. Electron Spectro. Relat. Phenom. **21**, 93–101 (1980)